A study on independently using static and dynamic light scattering methods to determine the coagulation rate

Hongwei Zhou, Shenghua Xu, Li Mi, Zhiwei Sun, and Yanming Qin

Citation: The Journal of Chemical Physics **141**, 094302 (2014); doi: 10.1063/1.4893876
View online: http://dx.doi.org/10.1063/1.4893876
View Table of Contents: http://scitation.aip.org/content/aip/journal/jcp/141/9?ver=pdfcov
Published by the AIP Publishing

A study on independently using static and dynamic light scattering methods to determine the coagulation rate

Hongwei Zhou,[1] Shenghua Xu,[1,a)] Li Mi,[1,2] Zhiwei Sun,[1,a)] and Yanming Qin[1,2]
[1]*Key Laboratory of Microgravity, Institute of Mechanics, Chinese Academy of Sciences, No.15 Beisihuanxi Road, Beijing 100190, People's Republic of China and National Microgravity Laboratory, Institute of Mechanics, Chinese Academy of Sciences, No.15 Beisihuanxi Road, Beijing 100190, People's Republic of China*
[2]*College of Chemistry, Chemical Engineering and Material Science, Shandong Normal University, Wenhua East Road 88, Jinan, Shandong 250014, People's Republic of China*

(Received 9 July 2014; accepted 12 August 2014; published online 2 September 2014)

Absolute coagulation rate constants were determined by independently, instead of simultaneously, using static and dynamic light scattering with the requested optical factors calculated by *T*-matrix method. The aggregating suspensions of latex particles with diameters of 500, 700, and 900 nm, that are all beyond validity limit of the traditional Rayleigh-Debye-Gans approximation, were adopted. The results from independent static and dynamic light scattering measurements were compared with those by simultaneously using static and dynamic light scattering; and three of them show good consistency. We found, theoretically and experimentally, that for independent static light scattering measurements there are blind scattering angles at that the scattering measurements become impossible and the number of blind angles increases rapidly with particle size. For independent dynamic light scattering measurements, however, there is no such a blind angle at all. A possible explanation of the observed phenomena is also presented. © *2014 AIP Publishing LLC*. [http://dx.doi.org/10.1063/1.4893876]

I. INTRODUCTION

Absolute coagulation rate constant (ACRC) is an important parameter for characterizing the stability and coagulation kinetics, which are two of the central problems in colloid science.[1,2] The relevant knowledge is also of great significance to several natural processes and technological applications,[3–8] such as pharmaceutical formulation, water and wastewater treatment, and material industries. Academically, ACRC plays an important role in understanding the mechanisms of colloidal stability and investigating fundamental inter-particle forces and hydrodynamic interactions.[9,10] It is also linked with the properties of colloidal suspensions.[2]

The coagulation rate has been studied both theoretically and experimentally for a long time. According to Smoluchowski theory ACRC for a rapid coagulation process is $8k_BT/3\eta$, where k_B is the Boltzmann constant, T is the temperature, and η is the viscosity.[11] However, the measured values of ACRC for rapid coagulation are generally much smaller than Smoluchowski's theoretical ones primarily because of the existence of the hydrodynamic interactions in practice.[12,13] And the ratio between the measured ACRC and the theoretical ones can be rather different for different systems. Moreover, for slow coagulation process the ACRC varies significantly depending on the nature of the dispersed phase and the dispersion medium. Therefore, it is a necessary and important step to measure the value of ACRC with certain accuracy in many cases. Accordingly, many efforts have been made to improve the measurement techniques of the coagulation rate.

In practice, the most commonly used approaches for determining coagulation rate are derived from the optical property changes of the dispersions during the coagulation process.[14–18] Specifically, turbidity measurement, static light scattering (SLS) and dynamic light scattering (DLS) are the most widely adopted methods. The major difficulty in determining coagulation rate by light scattering is how to theoretically calculate the so-called optical factor $I_2(q)/2I_1(q)$, where $I_1(q)$ and $I_2(q)$ (q is the scattering vector, see below for the definition) are the scattered intensity of a singlet and a doublet, respectively.

In the past, to evaluate the optical factor some approximations are available, such as commonly used Rayleigh-Debye-Gans (RDG) approximation,[19,20] that is applicable only to small particles under the condition of $\alpha|m-1| \ll 1$, where m is the relative refractive index of particles to medium and $\alpha = 2\pi a/\lambda$ is the size parameter (a is the particle radius and λ is the operating light wavelength).[21,22]

There have been some special efforts made in dealing with the optical factor of large particles, including the discrete dipole approximation (DDA)[23] modal analysis (MA).[24] Particularly, to bypass the difficulty in calculating the optical factor, the simultaneous static and dynamic light scattering (SSDLS) method was proposed and has successfully demonstrated its capability of determining the coagulation rates for large particles.[16]

On the other hand, the *T*-matrix method has great ability for accurately computing electromagnetic scattering by

a)Authors to whom correspondence should be addressed. Electronic addresses: xush@imech.ac.cn and sunzw@imech.ac.cn. Tel.: +86 1082544099. Fax: +86 10 82544096.

single and compounded spherical particles, without limits of size or shape.[25–27] The suitability of the *T*-matrix method was confirmed by comparing the experimentally obtained optical factors with that derived by the *T*-matrix method.[21] In turbidity measurement, we have effectively used *T*-matrix method in evaluating the extinction cross section of doublets to determine the coagulation rates of large sized particle dispersions.[14,15] It is supposed that if the *T*-matrix method is employed to achieve $I_2(q)/2I_1(q)$, either SLS or DLS method should be able to be used alone in determining the coagulation rates, instead of combining both of them.

Furthermore, turbidity measurement relies on the turbidity change of the dispersions caused by the aggregation of the dispersed particles. As previously shown, however, the degree of this change varies significantly with particle size and the operating wavelength. Particularly, at a certain wavelength (the so-called blind point), the change in turbidity completely loses its sensitivity to the coagulation process, which makes the measurement impossible. To acquire reliable coagulation rates, turbidity measurements should be performed at a wavelength some distance from the blind point.[14,28]

Considering the formula for evaluating coagulation rates by SLS and turbidity measurement are quite similar.[28] The only difference between them is that the variable in SLS formula is the scattering angle with the operating wavelength fixed while the variable in the turbidity formula is the wavelength with the angle fixed. So, it is expectable that there should also exist blind point of scattering angle in SLS method although no experimental verification has been observed yet.

In this study, we demonstrate that either SLS or DLS can independently determine coagulation rates for large sized particle dispersions with the aid of *T*-matrix in calculating the optical factor. From the results of different sized particles, we show, theoretically and experimentally, that the blind points of scattering angle exist for SLS measurements and the number of blind points increases rapidly with particle size. However, there is no blind point for DLS and SSDLS. We also provide an explanation for our findings. The results should provide useful clues for properly choosing methods and measurement parameters to improve the accuracy of measuring coagulation process in different cases.

II. BACKGROUND

A. Coagulation kinetics

The simplest coagulation kinetics for colloidal system is to study the early stage coagulation process when the dispersion is induced by some externally controlled parameters, such as the temperature or an electrolyte. At this stage, only collisions of single particles which form doublets need to be considered. Therefore, the change of particle number concentrations can be approximately expressed as[14,29]

$$\left(\frac{dN_1(t)}{dt}\right)_{t=0} = -k_{11}N_1(t)^2, \tag{1}$$

$$\left(\frac{dN_2(t)}{dt}\right)_{t=0} = \frac{1}{2}k_{11}N_1(t)^2, \tag{2}$$

where $N_1(t)$ and $N_2(t)$ are the number concentration of single particles and doublets, t is time, and k_{11} is coagulation rate.

B. Light scattering theory

1. Static light scattering

In the early stages of aggregation, the intensity of light scattered from a dilute suspension of coagulating monodisperse primary spheres is given by[16,30]

$$I(q,t) = N_1(t)I_1(q) + N_2(t)I_2(q), \tag{3}$$

where $I_1(q)$ and $I_2(q)$ are the scattered intensity of a singlet and a doublet, respectively. The scattering vector, q, is given by $q = (4\pi/\lambda)\sin(\theta/2)$, where λ is the wavelength of the light in the medium and θ is the scattering angle. Therefore,

$$\frac{dI(q,t)}{dt} = \frac{dN_1(t)}{dt}I_1(q) + \frac{dN_2(t)}{dt}I_2(q). \tag{4}$$

After inserting Eqs. (1) and (2), Eq. (4) becomes

$$\left[\frac{dI(q,t)}{dt}\right]_{t=0} = -k_{11}N_1(t)^2I_1(q) + \frac{1}{2}k_{11}N_1(t)^2I_2(q). \tag{5}$$

As a consequence,

$$k_{11} = \frac{[dI(q,t)/dt]_0/I(q,0)}{[I_2(q)/2I_1(q) - 1]N_0}, \tag{6}$$

where $I(q, 0)$ is the total scattering intensity at $t = 0$, and $I(q, 0) = N_0I_1(q)$ because only single particle exists in the system at this stage.

2. Dynamic light scattering

For DLS, one measures the average hydrodynamic radius of the particles and then the change of radius is used to evaluate coagulation rate. At the early stage of the aggregation, the averaged diffusion coefficient $\overline{D}$ measured by DLS can be expressed as[16]

$$\overline{D} = \frac{N_1(t)I_1(q)D_1 + N_2(t)I_2(q)D_2}{N_1(t)I_1(q) + N_2(t)I_2(q)}, \tag{7}$$

where D_1 and D_2 are the diffusion coefficients for single particle and doublet, respectively.

According to the Stokes–Einstein equation $D = k_BT/6\pi\eta r_h$, where k_B is the Boltzmann constant, T is the temperature, and η is the viscosity coefficient, Eq. (7) can be rewritten as

$$r_h(t) = \frac{N_1(t)I_1(q) + N_2(t)I_2(q)}{N_1(t)I_1(q)/r_{h,1} + N_2(t)I_2(q)/r_{h,2}}, \tag{8}$$

where $r_{h,1}$ and $r_{h,2}$ are the hydrodynamic radii of the singlet and doublet, respectively. At the beginning of aggregation, $r_{h,1} = r_h(0)$. Therefore,

$$\frac{r_h(t)}{r_h(0)} = \frac{r_h(t)}{r_{h,1}} = \frac{N_1(t)I_1(q) + N_2(t)I_2(q)}{N_1(t)I_1(q) + N_2(t)I_2(q)(r_{h,1}/r_{h,2})}. \tag{9}$$

Differentiating Eq. (9) with respect to t and inserting Eq. (1), we can finally get the expression of k_{11} in DLS

measurements

$$k_{11} = \frac{d[(r_h(t)/dt)/r_h(0)]_0}{(1 - r_{h,1}/r_{h,2})[I_2(q)/2I_1(q)]N_0}. \quad (10)$$

The relationship of $r_{h,1}$ and $r_{h,2}$, $r_{h,2} \cong 1.38r_{h,1}$, is calculated from the hydrodynamic forces of two spheres in a low Reynolds number fluid. If the two spheres are free to rotate, $r_{h,2} \cong 1.35r_{h,1}$.[16]

3. Simultaneous static and dynamic light scattering

To get around directly calculating or measuring the optical factor $I_2(q)/2I_1(q)$, Holthoff *et al.*[16,17] suggested that one can combined Eq. (6) for SLS and Eq. (10) for DLS, and then the coagulation rate can be written as

$$k_{11} = \frac{[d(r_h(t)/dt)/r_h(0)]_0}{(1 - r_{h,1}/r_{h,2})N_0} - \frac{[d(I(q,t)/dt)/I(q,0)]_0}{N_0}. \quad (11)$$

C. *T*-matrix method

According to Eqs. (6) and (10), for measuring the k_{11} by independent SLS or DLS method, one needs to evaluate the values of $I_2(q)$ and $I_1(q)$. Unlike commonly used RDG approximations that have size limitations, the *T*-matrix method can accurately compute electromagnetic scattering by single and compounded spherical particles without size limits, and even particles of other more complicated shapes. Therefore, in this study we use the *T*-matrix method to calculate $I_2(q)$ and $I_1(q)$.

In the *T*-matrix method, both incident and scattered electric fields are expanded in a series of vector spherical wave functions as follows:[19]

$$\mathbf{E}^{inc}(\mathbf{r}) = \sum_{n=1}^{\infty}\sum_{m=-n}^{n}[a_{mn}Rg\mathbf{M}_{mn}(kr) + b_{mn}Rg\mathbf{N}_{mn}(kr)], \quad (12)$$

$$\mathbf{E}^{sca}(\mathbf{r}) = \sum_{n=1}^{\infty}\sum_{m=-n}^{n}[p_{mn}\mathbf{M}_{mn}(kr) + q_{mn}\mathbf{N}_{mn}(kr)], \quad (13)$$

where $k = 2\pi/\lambda$ and λ is the wavelength. Due to the linearity of Maxwell's equations, the scattered field coefficients $\mathbf{p} = [p_{mn}, q_{mn}]$ are related to the incident field coefficients $\mathbf{a} = [a_{mn}, b_{mn}]$ by means of the so-called transmission matrix (or *T*-matrix)

$$p_{mn} = \sum_{n'=1}^{\infty}\sum_{m'=-n'}^{n'}\left[T^{11}_{mnm'n'}a_{m'n'} + T^{12}_{mnm'n'}b_{m'n'}\right], \quad (14)$$

$$q_{mn} = \sum_{n'=1}^{\infty}\sum_{m'=-n'}^{n'}\left[T^{21}_{mnm'n'}a_{m'n'} + T^{22}_{mnm'n'}b_{m'n'}\right]. \quad (15)$$

In compact matrix notation, Eqs. (14) and (15) can be rewritten as

$$\begin{bmatrix}\mathbf{p}\\ \mathbf{q}\end{bmatrix} = \mathbf{T}\begin{bmatrix}\mathbf{a}\\ \mathbf{b}\end{bmatrix} = \begin{bmatrix}\mathbf{T^{11}} & \mathbf{T^{12}}\\ \mathbf{T^{21}} & \mathbf{T^{22}}\end{bmatrix}\begin{bmatrix}\mathbf{a}\\ \mathbf{b}\end{bmatrix}, \quad (16)$$

which means that the column vector of the expansion coefficients of the scattered field is obtained by multiplying the *T*-matrix and the column vector of the expansion coefficients of the incident field.

Consider now the computation of the *T*-matrix for a cluster consisting of *N* spheres. The total scattered electric field can be written as the sum of the fields scattered by all spheres,

$$\mathbf{E}^{sca}(\mathbf{r}) = \sum_{j=1}^{N}\mathbf{E}_j^{sca}(\mathbf{r}). \quad (17)$$

And the total electric field exciting each particle can be written as the sum of the external incident field $\mathbf{E}_0{}^{\text{inc}}(\text{r})$ and the partial fields scattered by all other particles,

$$\mathbf{E}_j^{inc}(\mathbf{r}) = \mathbf{E}_0^{inc}(\mathbf{r}) + \sum_{\substack{l=1\\ l\neq j}}^{N}\mathbf{E}_l^{inc}(\mathbf{r}) \quad j = 1, 2, \ldots, N. \quad (18)$$

The field scattered by the *l*th particle can also be expanded in outgoing vector spherical wave functions entered at the origin of the *l*th local coordinate system,

$$\mathbf{E}_l{}^{sca}(\mathbf{r}) = \sum_{\nu=1}^{\infty}\sum_{\mu=-\nu}^{\nu}\left[p^l_{\mu\nu}\mathbf{M}_{\mu\nu}(kr_l) + q^l_{\mu\nu}\mathbf{N}_{\mu\nu}(kr_l)\right]. \quad (19)$$

As shown in Ref. 19, the vector spherical wave functions appearing here can be expanded in regular vector spherical wave functions centered at the origin of the *j*th reference frame,

$$\mathbf{M}_{\mu\nu}(k\mathbf{r}_l) = \sum_{\nu=1}^{\infty}\sum_{\mu=-\nu}^{\nu}[A_{mn\mu\nu}(k\mathbf{r}_{lj})Rg\mathbf{M}_{mn}(k\mathbf{r}_j) + B_{mn\mu\nu}(k\mathbf{r}_{lj})Rg\mathbf{N}_{mn}(k\mathbf{r}_j)], \quad (20)$$

$$\mathbf{N}_{\mu\nu}(k\mathbf{r}_l) = \sum_{\nu=1}^{\infty}\sum_{\mu=-\nu}^{\nu}[B_{mn\mu\nu}(k\mathbf{r}_{lj})Rg\mathbf{M}_{mn}(k\mathbf{r}_j) + A_{mn\mu\nu}(k\mathbf{r}_{lj})Rg\mathbf{N}_{mn}(k\mathbf{r}_j)], \quad (21)$$

where the vector $\mathbf{r}_{lj} = \mathbf{r}_l - \mathbf{r}_j$. The explicit expressions for the translation coefficients $A_{mn\mu\nu}(k\mathbf{r}_{lj})$ and $B_{mn\mu\nu}(k\mathbf{r}_{lj})$ can be found in Ref. 19. Then the expression for $\mathbf{p}^j$ and $\mathbf{q}^j$ can be derived in matrix notation,

$$\begin{bmatrix}\mathbf{p}^j\\ \mathbf{q}^j\end{bmatrix} = \mathbf{T}^j\left(\begin{bmatrix}\mathbf{a}^{j0}\\ \mathbf{b}^{j0}\end{bmatrix} + \sum_{l\neq j}\begin{bmatrix}\mathbf{A}(k\mathbf{r}_{lj}) & \mathbf{B}(k\mathbf{r}_{lj})\\ \mathbf{B}(k\mathbf{r}_{lj}) & \mathbf{A}(k\mathbf{r}_{lj})\end{bmatrix}\begin{bmatrix}\mathbf{p}^l\\ \mathbf{q}^l\end{bmatrix}\right) = \mathbf{T}^j\left(\mathbf{a}^{j0} + \sum_{l\neq j}\mathbf{A}^{jl}\mathbf{p}^l\right), \quad (22)$$

where $\mathbf{T}^j$ represents the *T*-matrix for the particle *j*, when isolated. Inversion of Eq. (22) gives sphere-centered transition matrices that transform the expansion coefficients of the incident field into expansion coefficients of the individual scattered fields,

$$\begin{bmatrix}\mathbf{p}^j\\ \mathbf{q}^j\end{bmatrix} = \sum_{l=1}^{N}\mathbf{T}^{jl}\begin{bmatrix}\mathbf{a}^{l0}\\ \mathbf{b}^{l0}\end{bmatrix} \quad j = 1, 2, \ldots, N. \quad (23)$$

Finally, the scattered field expansions from the individual spheres will be transformed into a single expansion based on a single origin of the particle system. The incident and scattered coefficients for the system will be derived as

$$\begin{bmatrix} \mathbf{p} \\ \mathbf{q} \end{bmatrix} = \sum_j \begin{bmatrix} \mathbf{p}^j \\ \mathbf{q}^j \end{bmatrix} = \sum_{j,i} \mathbf{B}^j \mathbf{T}^{ji} \begin{bmatrix} \mathbf{a}^i \\ \mathbf{b}^i \end{bmatrix} = \sum_{j,i} \mathbf{B}^j \mathbf{T}^{ji} \mathbf{B}^i \begin{bmatrix} \mathbf{a} \\ \mathbf{b} \end{bmatrix}$$
$$= \mathbf{T} \begin{bmatrix} \mathbf{a} \\ \mathbf{b} \end{bmatrix} = \begin{bmatrix} \mathbf{T^{11}} & \mathbf{T^{12}} \\ \mathbf{T^{21}} & \mathbf{T^{22}} \end{bmatrix} \begin{bmatrix} \mathbf{a} \\ \mathbf{b} \end{bmatrix}, \quad (24)$$

where the **B** matrices are similar to the **A** matrices of Eq. (22). Now, the matrix **T** so defined in Eq. (24) is the one needed for the calculations of light-scattering properties of the aggregated particle system. For calculation of $I_2(q)$ and $I_1(q)$ in this study, N will be chosen to be 2 and 1, respectively.

From the calculated T-matrix, the Stokes scattering matrix which transforms the Stokes vector of incident light to that of scattering light, can be deduced accordingly. And the scattered intensities $I_2(q)$ and $I_1(q)$ can be directly obtained from the Stokes vector of the scattering light for doublet and singlet. More details can be found in Refs. 19, 25–27, and 31.

III. EXPERIMENTAL

Since practice has shown that the SSDLS approach is feasible, we take the coagulation rates achieved by SSDLS as references to assess the results obtained by independently using SLS and DLS with the requested optical properties calculated by T-matrix method in different cases.

A. Materials

Three kinds of polystyrene (PS) latex particles (3000 series) purchased from Duke Scientific Corporation were used in this study. The diameters are 500 nm (coefficient of variation 1.6%), 700 nm (coefficient of variation 1.2%) and 900 nm (coefficient of variation 0.5%), and they were assigned as PS500, PS700, and PS900, respectively. The densities for these particles are 1.05 g/cm^3 and their solid content concentrations are 1.0% according to the information provided by the manufacturer.

B. Instrument

A Brookhaven light scattering device composed of a BI-200SM goniometer, a BI-9000AT digital correlator, and a photomultiplier detector were used in this study for static and dynamic light scattering experiments. The light source is a 200 mW solid-state laser operating at a wavelength of 532 nm (MGL-III-532, CNI). The measurement temperature was controlled by a thermostatic circulator (LTD6G, Grant) with an accuracy of ±0.05 °C.

C. Methods

Before the measurements were started, the containers for the electrolyte and latex solutions as well as the sample cells were cleaned with a chromium sulfuric acid solution and then rinsed excessively with de-ionized water in order to eliminate organic materials. The use of any detergent-based cell-cleaning solution was avoided because the coagulation rate is sensitive to the presence of trace amounts of surfactants. The de-ionized water was obtained from an ultra-pure water treatment apparatus (UPRLCDRO, RELATEC), and the resistivity is larger than 16 MΩ cm. The samples were prepared by diluting the stock suspensions with de-ionized water. The initial particle number concentration was determined according to the particle size and dry weight of the dispersions of a certain amount of the sampling solution. The estimated error associated with the number concentration is about 5%.

In a typical procedure of light scattering experiment, 8 ml sample solution in the cell was mixed with 8 ml of 1.5 M NaCl solution. The salt concentration in the mixture is 0.75 M, and it is sufficiently higher than the required critical coagulation concentration to induce fast aggregation. After the cell was gently shaken, the coagulation process was monitored by time-resolved light scattering.

IV. EXPERIMENTAL RESULTS AND DISCUSSIONS

A. SLS measurements

Using Eq. (6) to get the coagulation rate by SLS method, one needs to calculate $I_2(q)/2I_1(q) - 1$ from the measurement of scattering light change during aggregation. In this study, $I_2(q)/2I_1(q) - 1$ at different scattering angles were calculated by using T-matrix method.

As mentioned above, for turbidity measurement there may be blind point for the operating wavelength at which the turbidity will not change during aggregation, because the extinction cross section of two singlets is just equal to that of one doublet.[14] Since the formula for evaluating coagulation rates in SLS measurement have quite similar formation as that used in turbidity measurement, we believed that the blind points would also exist in SLS method. These blind points will be the angles (blind angles), instead of the wavelength for the turbidity measurement, that make $I_2(q)/2I_1(q) - 1$ equal to zero so that $dI(q, t)/dt$ will also be zero correspondingly.

The calculated $I_2(q)/2I_1(q) - 1$ of PS500 using T-matrix method was shown in Fig. 1(a). There are five angles where $I_2(q)/2I_1(q) - 1$ equals to zero. As typical examples, we investigated the change tendency of scattering light $dI(q, t)/dt$ at three of them, 46°, 75°, and 104°. The results show that the intensity of the scattering light is basically unchanged during the coagulation process at all the three angles (see Fig. 2), which is consistent with the theoretical calculation and verifies that they are the blind angles that both $I_2(q)/2I_1(q) - 1$ and $dI(q, t)/dt$ are close to zero. However, for angle 90°, which approximately located at the middle of two adjacent blind angles 75° and 104°, the change tendency of scattering light is observable. In addition, the negative slope of $dI(q, t)/dt$ is also in accordance with the sign of the calculated $I_2(q)/2I_1(q) - 1$ at 90°. Similar to the turbidity measurements, we should also avoid performing SLS measurements near the blind angles, to enhance the signal-to-noise ratio and reduce the uncertainties in the measurements.

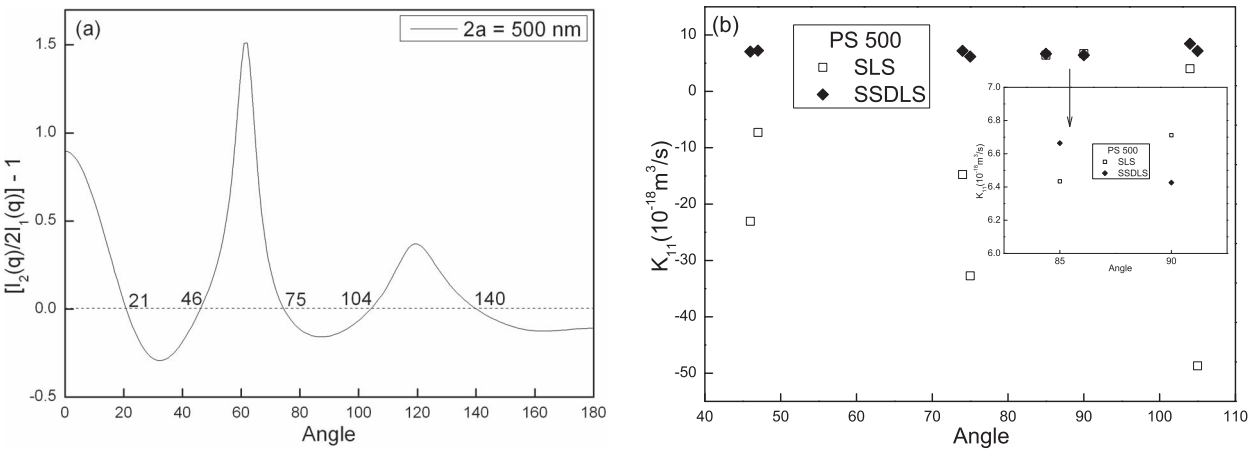

FIG. 1. (a) The calculated optical factor of particles with 500 nm diameter through *T*-matrix method. (b) Comparisons between the results of independent SLS and SSDSL for PS500 dispersions with $N_1 = 5 \times 10^{13}$ m^{-3}. Inset: Enlarged picture showing the results of SLS and SSDLS obtained at 85° and 90°.

In order to further examine the influence of these blind angles, we measured coagulation rates at these three blind angles (46°, 75°, 104°) and their adjacent regions (47°, 74°, 105°), and compared the results with two other angles (85°, 90°) located away from these blind angles (see Fig. 1(b)). And all the obtained results were compared correspondingly with the values obtained from SSDLS method, which has been proved to be able to get the reasonable coagulation rates. Some preliminary conclusions can be drawn. First, at the blind angles and in their adjacent regions, the coagulation rates obtained from SLS and SSDLS fluctuated drastically and most of the SLS values are even meaninglessly negative.

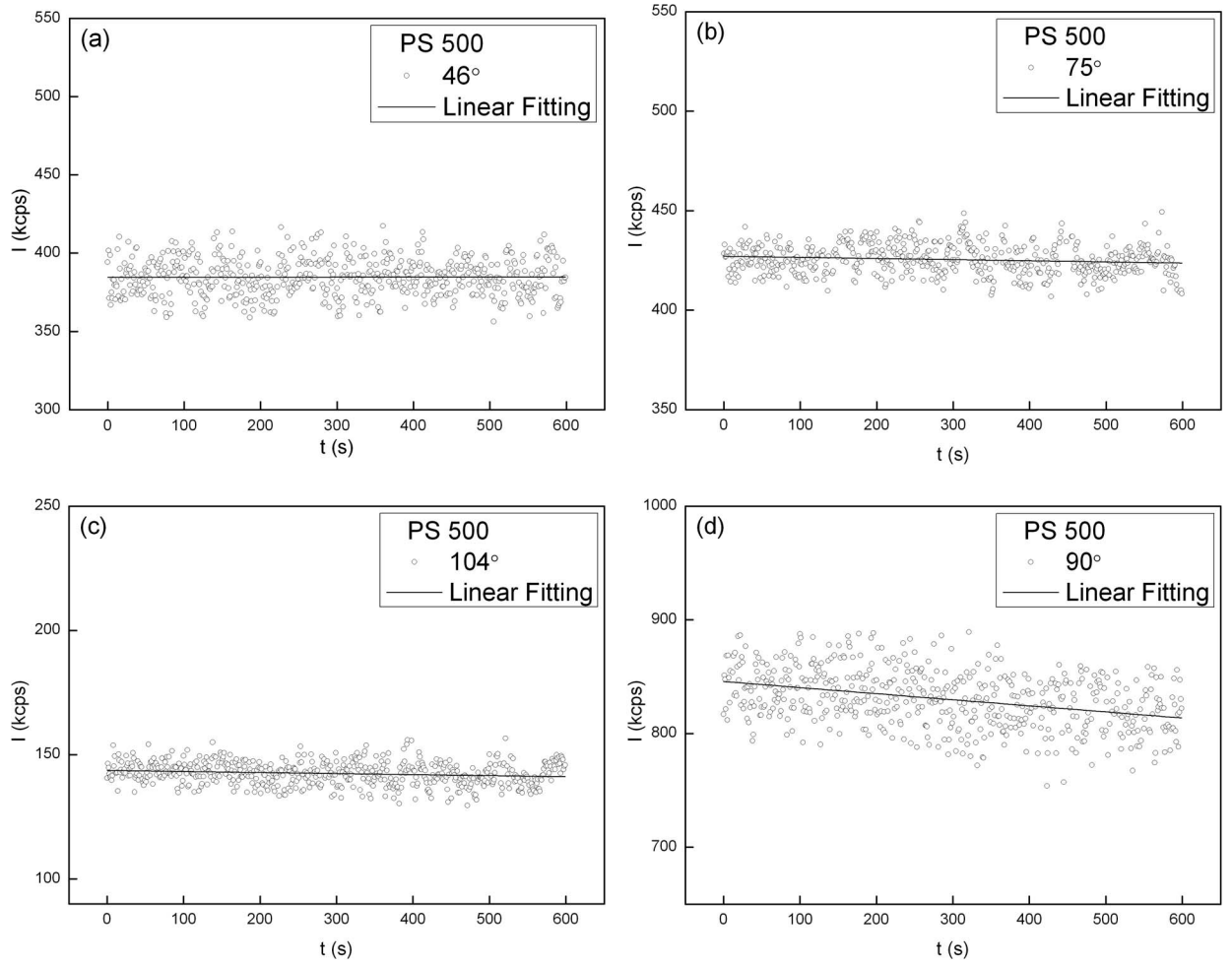

FIG. 2. The change tendency of scattering light intensity measured at three blind angles, (a) 46°, (b) 75°, (c) 104° and one non-blind angle, (d) 90°, in the coagulation process of PS500 dispersions.

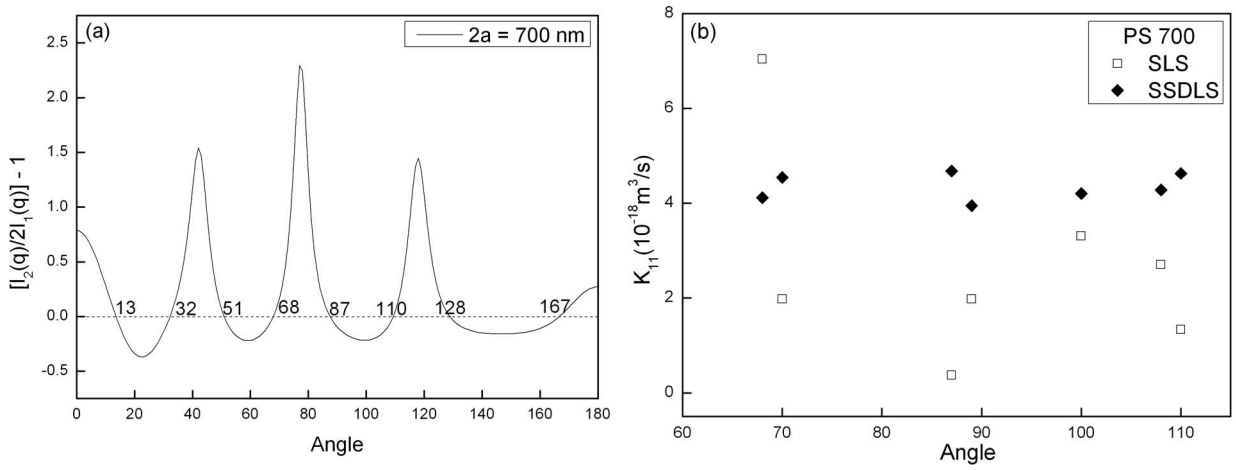

FIG. 3. (a) The calculated optical factor of particles with 700 nm diameter through *T*-matrix method. (b) Comparisons between the results of independent SLS and SSDSL for PS700 dispersions with $N_1 = 5 \times 10^{13}$ m^{-3}.

This is because the absolute value of d*I*/d*t* is too low to be correctly measured in this low signal-noise ratio region. And even a small measurement error caused by large noise might result in a reverse sign of d*I*/d*t* comparing with its real value. Second, at the two angles 85° and 90°, that are a distance away from the blind angles (at least 10° difference), coagulation rates obtained from SLS and SSDLS are pretty close (see Fig. 1(b) and the inset). Quantitatively, at 85°, the coagulation rates are 6.4×10^{-18} m^3 s^{-1} (SLS) and 6.7×10^{-18} m^3 s^{-1} (SSDLS). And at 90°, the values are 6.7×10^{-18} m^3 s^{-1} (SLS) and 6.4×10^{-18} m^3 s^{-1} (SSDLS), respectively. Therefore, the results show that the SLS method can independently measure the coagulation rates with the aid of *T*-matrix calculation for the required optical factor, but, the angles near the blind angles should be avoided.

The situation for PS700 is basically similar to that for PS500 described above. The differences between coagulation rates of SLS and SSDLS measured at three blind angles (68°, 87°, 110°) and their adjacent regions (70°, 89°, 108°) are huge. On the other hand, such differences measured at 100°, which is respectively 13° and 10° away from the two adjacent blind angles 87° and 110°, are less than 12% of the average value of SSDLS (see Fig. 3(b)). However, for PS900, since there are more blind angles appeared it is hardly possible to find any angle to have no blind angle nearby. So all the results of SLS deviate from the value of SSDLS are unacceptably large no matter at which angle the measurement was performed (see Fig. 4(b), please note the scale of y axis). Even at 102°, an angle located at the middle of two blind angles (90° and 111°), the deviation of SLS's data from that of SSDLS is still more than two times larger than the average value of SSDLS.

Although there are blind angles for all the samples of three different sized particles, the occurrence frequency of blind angles is different. For PS500, there are five blind angles (see Fig. 1(a)). But with the increase of particle diameter, the number of blind angles increases, which is eight for PS700 (see Fig. 3(a)) and ten for PS900 (see Fig. 4(a)), respectively. Apparently, as shown above, with the increasing number of blind angles, actually, there is simply no way to find an angle which is at least 10° away from the blind angles. This is why we can get reasonable coagulate rates by independently using

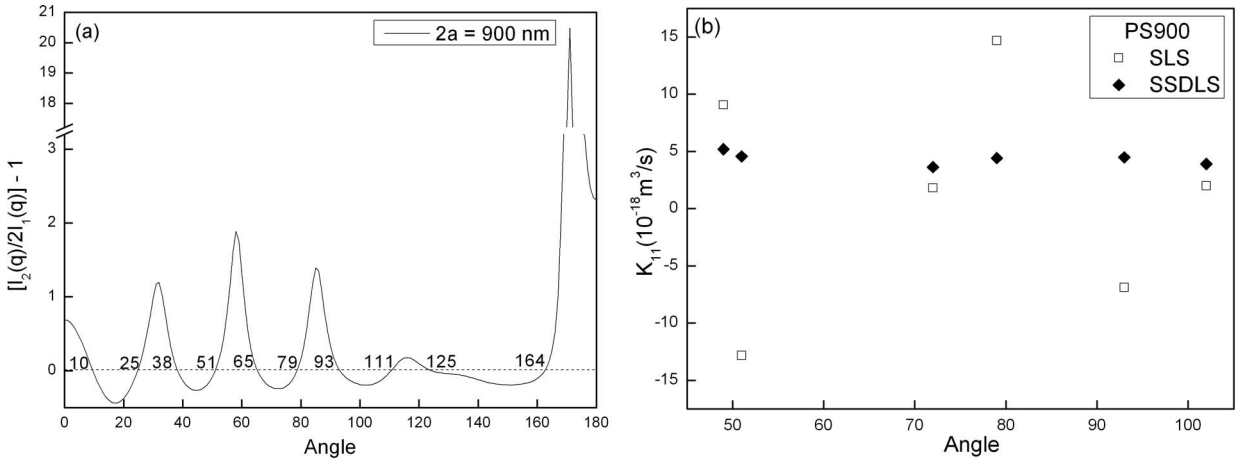

FIG. 4. (a) The calculated optical factor of particles with 900 nm diameter through *T*-matrix method. (b) Comparisons between the results of independent SLS and SSDSL for PS900 dispersions with $N_1 = 2 \times 10^{13}$ m^{-3}.

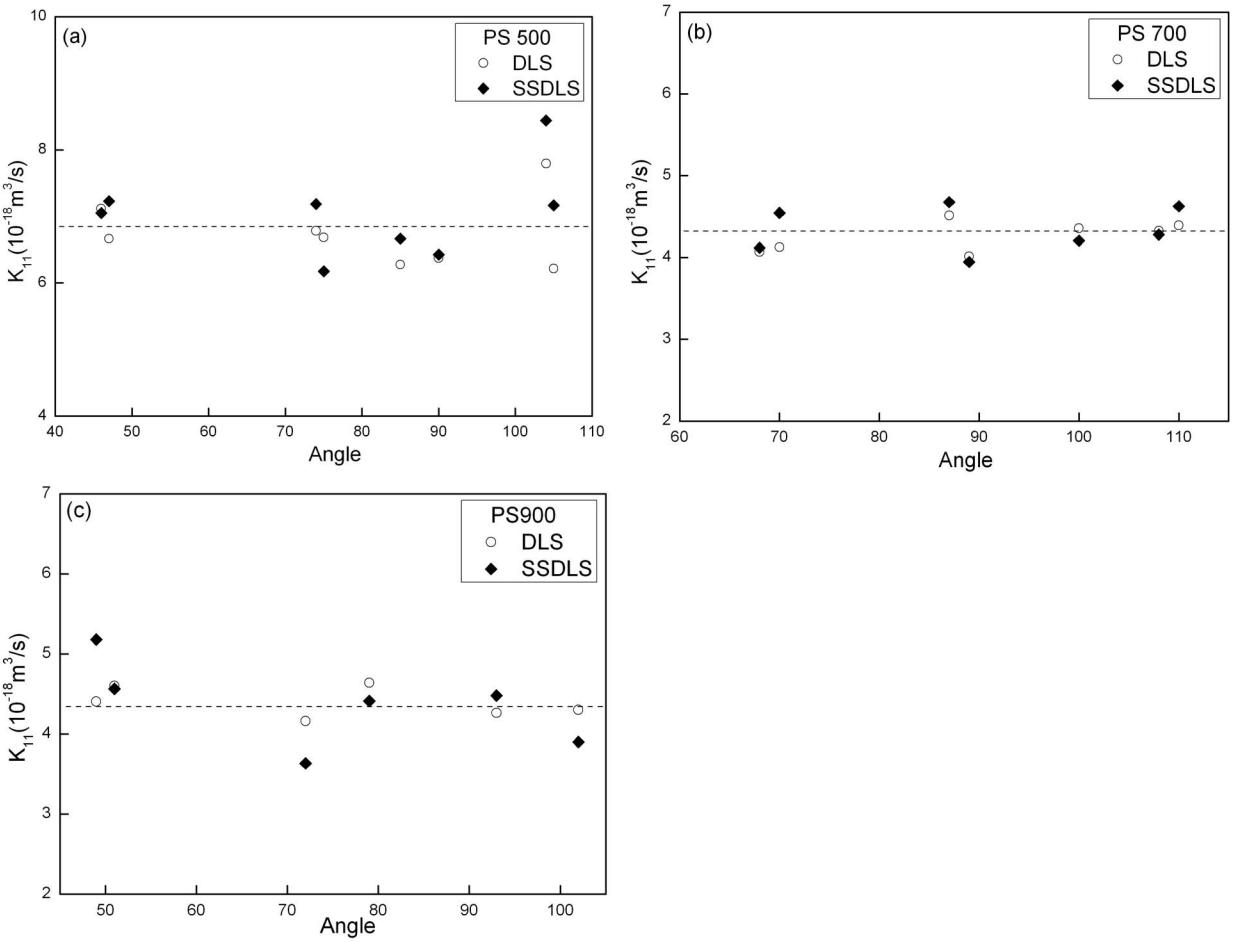

FIG. 5. The measured K_{11} obtained from independent DLS and SSDLS measurements. The concentration of the dispersions is the same as that used in SLS measurements correspondingly. (a) PS500, (b) PS700, and (c) PS900.

SLS method at two angles (85° and 90°) for PS500, but there is only one acceptable angle for PS700 (100°) and no proper angle for PS900.

Figs. 1(a) and 3(a)–4(a) present the calculated distribution of blind angles and the changes of $I_2(q)/2I_1(q) - 1$ at different scattering angles. From these figures, it is possible to choose "optimal angles" for the measurement of coagulation rate by independent SLS. These angles should be at a certain distance, such as 10°, from the blind angles to ensure a good contrast between one dimmer scattering ($I_2(q)$) and two primary scattering ($2I_1(q)$) intensities. However, this does not mean that the angle with larger absolute value of $I_2(q)/2I_1(q) - 1$ is better. Since the measurement angle may have some error, one should also choose angles around which the value of $I_2(q)/2I_1(q) - 1$ changes slowly for ensuring a high error tolerance. For examples in Fig. 3(a), the absolute value of $I_2(q)/2I_1(q) - 1$ is largest at angle 77°, but 1° difference can result in an error of $I_2(q)/2I_1(q) - 1$ about 20%. For angles 75° or 79°, the error can be 40% for 1° difference. Comparatively, around 100° which was used in our previous discussion, the error is only 2% for 1° difference. Therefore, in above discussions, the angles used to compare with the blind angles were all at the valleys of the curves. From both experimental results and analyses, it can be concluded that the "optimal angles" for SLS measurement should be at more than 10° from the blind angles and also in the range that $I_2(q)/2I_1(q) - 1$ changes slowly with angle. At these "optimal angles," the independent SLS approach is technically feasible for measuring coagulation rates with certain accuracy for large sized particle dispersions.

B. DLS measurements

Similar to SLS measurement, the coagulation rates can also be determined from independent DLS measurement according to Eq. (10) with the known $I_2(q)/2I_1(q)$, which have already been calculated in SLS measurement mentioned in Sec. IV A. However, there is a key difference between DLS and SLS method. For SLS method, there are blind angles because the denominator in Eq. (6) can be zero, but for DLS method, all the terms of the denominator in Eq. (10) are positive and will not have a chance to be zero, which means no blind angle in DLS measurement. That is, the independent DLS method should be able to be used at any scattering angles.

Toward this end, we measured the coagulation rates by DLS method at different angles including blind angles for SLS method. The results are also compared with those of SSDLS (see Fig. 5). For each kind of the three different sized particles, we found the values of coagulation rates measured

at different angles by DLS method are close, and they are also close to those obtained by SSDLS method.

Quantitatively, we averaged the coagulation rates of DLS and SSDLS for comparisons. For PS500, the averaged value measured by DLS is 6.7×10^{-18} m^3 s^{-1} and it is 6.9×10^{-18} m^3 s^{-1} by SSDLS. The results are similar for the other two kinds of dispersions. For PS700, coagulation rates obtained by DLS and SSDLS are 4.2×10^{-18} m^3 s^{-1} and 4.3×10^{-18} m^3 s^{-1}, respectively. And for PS900, coagulation rates obtained by DLS and SSDLS are 4.4×10^{-18} m^3 s^{-1} and 4.5×10^{-18} m^3 s^{-1}, respectively. Therefore, our experiments showed that DLS can independently determine the coagulation rates of large sized particles after $I_2(q)/2I_1(q)$ was calculated by *T*-matrix method. Additionally, unlike the independent SLS method, there is no blind angle in DLS method.

For better understanding why the measured results by DLS method is so close to SSDLS method at all angles, we further analyzed the equations used in DLS and SSDLS method. The Eq. (10) for DLS method can be rewritten as

$$k_D = \frac{d[(r_h(t)/dt)/r_h(0)]_0}{(1 - r_{h,1}/r_{h,2})N_1} - [I_2(q)/2I_1(q) - 1]k_D, \quad (25)$$

while Eq. (11) for SSDLS method can be rewritten as

$$k_{SD} = \frac{d[(r_h(t)/dt)/r_h(0)]_0}{(1 - r_{h,1}/r_{h,2})N_1} - [I_2(q)/2I_1(q) - 1]k_S, \quad (26)$$

where we use k_S, k_D, and k_{SD} to distinguish the measured coagulation rates by SLS, DLS, and SSDLS, respectively. And the deduction of Eq. (26) has used Eq. (6) for SLS method.

The only difference between Eqs. (25) and (26) is that the coagulation rate in the second term is k_D (DLS measured value) for DLS method and k_S (SLS measured value) for SSDLS method. If the measurement is done at angles far away from the blind angles for SLS method, the results of both SLS and DLS should approach the actual value of the coagulation rates within an allowable total error range. In this case we will have $k_S \approx k_D$. Therefore, k_D from Eq. (25) will be almost equal to k_{SD} from Eq. (26) under this condition. On the other hand, if the measurement is performed at angles near the blind angles, the measured k_S will lose its accuracy and deviate from k_D. However, in the region near a blind angle, $I_2(q) \approx 2I_1(q)$, that is $[I_2(q)/2I_1(q) - 1] \approx 0$. This means that the influence of the difference between k_D and k_S (in the second term of Eqs. (25) and (26)) on the results of k_D and k_{SD} at the left hand of Eqs. (25) and (26) becomes ignorable. And this is the reason why the measured k_D and k_{SD} will also be close even for angles near the blind angles of SLS.

A physical interpretation for the reason why SLS has blind angles but DLS does not is offered below. SLS measurement of the coagulation rate relies on the change in scattering light intensity when two singlets form one doublet. It is possible at certain angle to have the summed light intensity scattered by two singlets ($2I_1(q)$) to be equal to the intensity scattered by one doublet ($I_2(q)$). In this case, SLS measurement becomes impossible. On the other hand, DLS measurement depends on the change in the average hydrodynamic radius of the particles during the coagulation process. As long as the coagulation process is ongoing, the average hydrodynamic radius always increases no matter at what angle the DLS measurement is performed. Actually the factor $(1 - r_{h,1}/r_{h,2})$ has nothing to do with measuring angle. In other words, there is no so-called blind angle for DLS measurement.

V. CONCLUSION

In this study we conduct an investigation on the determination of the absolute coagulation rate constant by independently using static and dynamic light scattering with the optical factor calculated by *T*-matrix method. The particle diameters are 500, 700, and 900 nm in the experiments and all these particles exceed the upper limit of validity of the traditional RDG approximation. Coagulation rates from independent SLS and DLS measurements are compared with those from SSDLS method. The main results of this study can be summarized as follows.

In accordance with the previous consideration, our experiments confirmed the existence of blind angles in independent SLS measurement. At those angles and their vicinities, SLS measurement becomes impossible because optical factor $I_2(q)/2I_1(q) - 1 \approx 0$, namely the scattered light has no reaction to the aggregation process. This fact suggests that the SLS measurement should be performed at the angles staying away from the blind angles. We further showed that the number of blind angles increases with the increasing of particle diameter, indicating that for larger particles, the SLS measurement becomes more difficult. As a result, carefully selecting the scattered light acceptance angle is a prerequisite of the success of determination of coagulation rates by independently SLS method.

For independent DLS measurement, on the other hand, there is no blind angle. Therefore, independent DLS is rather robust approach for determining the coagulation rates.

The reason why SLS has blind angles but DLS does not is that the former relies on the changes of scattering light intensity that depends on the scattering angle and the latter on the changes of hydrodynamic radius which has nothing to do with the scattering angle.

Comparing all the methods discussed above concerning the blind point, it would be interesting to see that DLS and SSDLS methods have 0 blind point (the variable is angle); turbidity method has 1 blind point (its variable is the wavelength) and SLS has many blind points and its number increases with particle size.

ACKNOWLEDGMENTS

This work is supported by Grant Nos. 11302226, 10972217, and 11032011 from the National Natural Science Foundation of China (NNSFC).

[1]M. Elimelech, J. Gregory, X. Jia, and R. A. Williams, *Particle Deposition and Aggregation: Measurement, Modeling and Simulation* (Butterworth-Heinemann, Oxford, U.K., 1995).
[2]J. Gregory, Adv. Colloid Interface Sci. **147–148**, 109 (2009).
[3]P. Vera, V. Gallardo, J. Salcedo, and A. V. Delgado, J. Colloid Interface Sci. **177**, 553 (1996).
[4]J. L. Arias, A. Gomez-Gallo, A. V. Delgado, and V. Gallardo, Colloid Surf. A-Physicochem. Eng. Asp. **338**, 107 (2009).
[5]Y. P. Duan, X. Z. Meng, Z. H. Wen, R. H. Ke, and L. Chen, Sci. Total Environ. **447**, 267 (2013).

[6]J. H. Zhang, Z. Q. Sun, and B. Yang, Curr. Opin. Colloid Interface Sci. **14**, 103 (2009).
[7]J. X. Wang, Y. Z. Zhang, S. T. Wang, Y. L. Song, and L. Jiang, Acc. Chem. Res. **44**, 405 (2011).
[8]R. K. Shah, J. W. Kim, and D. A. Weitz, Langmuir **26**, 1561 (2010).
[9]Y. Matsuoka, T. Fukasawa, K. Higashitani, and R. Yamamoto, Phys. Rev. E **86**, 051403 (2012).
[10]J. M. Lopez-Lopez, A. Schmitt, A. Moncho-Jorda, and R. Hidalgo-Alvarez, Soft Matter **2**, 1025 (2006).
[11]M. von Smoluchowski, Phys. Z. **17**, 557 (1916).
[12]L. A. Spielman, J. Colloid Interface Sci. **33**, 562 (1970).
[13]L. B. Brakalov, Chem. Eng. Sci. **42**, 2373 (1987).
[14]Z. W. Sun, J. Liu, and S. H. Xu, Langmuir **22**, 4946 (2006).
[15]J. Liu, S. Xu, and Z. Sun, Langmuir **23**, 11451 (2007).
[16]H. Holthoff, S. U. Egelhaaf, M. Borkovec, P. Schurtenberger, and H. Sticher, Langmuir **12**, 5541 (1996).
[17]H. Holthoff, A. Schmitt, A. FernandezBarbero, M. Borkovec, M. A. CabrerizoVilchez, P. Schurtenberger, and R. HidalgoAlvarez, J. Colloid Interface Sci. **192**, 463 (1997).
[18]K. Wang, A. K. Singh, and J. H. van Zanten, Langmuir **18**, 2421 (2002).
[19]M. I. Mishchenko, L. D. Travis, and A. A. Lacis, *Scattering, Absorption, and Emission of Light by Small Particles* (Cambridge University Press, Cambridge, U.K., 2002).
[20]C. Bohren and D. R. Huffman, *Absorption and Scattering of Light by Small Particles* (Wiley Interscience, New York, 1983).
[21]P. Galletto, W. Lin, M. I. Mishchenko, and M. Borkovec, J. Chem. Phys. **123**, 064709 (2005).
[22]H. Holthoff, M. Borkovec, and P. Schurtenberger, Phys. Rev. E **56**, 6945 (1997).
[23]B. T. Draine and P. J. Flatau, J. Opt. Soc. Am. A **11**, 1491 (1994).
[24]D. W. Mackowski, Proc. R. Soc. London, Ser. A **433**, 599 (1991).
[25]D. W. Mackowski and M. I. Mishchenko, J. Opt. Soc. Am. A **13**, 2266 (1996).
[26]M. I. Mishchenko and D. W. Mackowski, Opt. Lett. **19**, 1604 (1994).
[27]M. I. Mishchenko, J. Opt. Soc. Am. A **8**, 871 (1991).
[28]S. Xu and Z. Sun, Soft Matter **7**, 11298 (2011).
[29]M. von Smoluchowski, Z. Phys. Chem. **92**, 129 (1917).
[30]M. Berka and J. A. Rice, Langmuir **20**, 6152 (2004).
[31]See http://www.giss.nasa.gov/staff/mmishchenko/t_matrix.html for the relevant source codes of *T*-matrix.